Fabrication of Nanoscale Magnetic Domains Using Block-Copolymer Lithography

by

Babajide Akinronbi

Submitted to the Department of Materials Science and Engineering in Partial Fulfillment of the Requirements for the Degree of

Bachelor of Science

at the Massachusetts Institute of Technology

May 2014
[June 2014]

Signature of Author Signature redacted
Department of Materials Science & Engineering
May 2, 2014

Certified by Signature redacted
Caroline Ross
Toyota Professor of Materials Science & Engineering
Thesis Supervisor

Accepted by Signature redacted
Jeffrey C. Grossman
Professor of Computational Materials Science
Chair of the Undergraduate Committee

Fabrication of Nanoscale Magnetic Domains Using Block-Copolymer Lithography

by

Babajide Akinronbi

Submitted to the Department of Materials Science & Engineering on May 2, 2014
In Partial Fulfillment of the Requirements for the Degree of Bachelor of Science in Materials Science and Engineering

Abstract

The tendency of PS-b-PDMS to phase separate, the tunability of the resulting morphology and the sufficient etch contrast between PS and PDMS makes the block copolymer ideal for creating patterns that can be transferred onto magnetic media. The aim of this study was to determine optimal BCP film thicknesses that produce spherical micro-domains with long range order on a Co substrate brushed with PS-OH and to transfer this pattern onto the underlying Co. Thin films of PS-b-PDMS were spun-cast onto Co substrates brushed with PS-OH, solvent annealed and consequently etched in a series of steps that removed one constituent polymer at a time. Patterns with periods between 36-39nm and with great long-range order were observed for BCP film thicknesses in the 32-35 nm range and successful transfer of the pattern onto Co film was achieved, resulting in fabrication of nanoscale, discrete domains.

Table of Contents

List of Figures

Page Numbers:

List of Tables

Acknowledgements:

Much thanks to Professor Caroline Ross for providing me with the opportunity to conduct research in her lab on a topic that I found particularly engaging. I appreciate her guidance and willingness to help. I would also like to thank Kun-Hua Tu for his continued support and guidance over the course of my project. I owe much of the success of this project to him.

1. Introduction

1.1 Background

One of the hallmarks of the digital age is an ever- increasing insatiable appetite for data and consequently an ever-increasing need to store more data. From the internet corporations interested in the browsing behavior of visitors to the typical modern teenager carrying mobile devices that practically function as mini-computers, there has been a dramatic change in the sheer volume of available data. As a result, there is a pressing technological need to develop devices with significantly more storage capacity than traditional devices.

Even though there are many components in a data storage device, the part responsible for data storage in traditional devices is a magnetic Co alloy layer[1] – depicted in Figure 1.A single bit of memory consists of adjacent, similarly magnetized grains. For instance, a typical bit could span a 20 nm x by 80 nm area. [1] With this design, a read-write head detects differences in magnetization across the magnetic layer. It also magnetizes grains appropriately when data is written onto the layer. A dramatic shift in grain magnetization across a grain boundary corresponds to a '1' in the binary system while an unchanged magnetization corresponds to a '0'.

The active layer is often deposited on a substrate at a high temperature so as to facilitate the diffusion of non-magnetic elements to the grain boundaries. These nonmagnetic elements act as a barrier to minimize exchange coupling between individual grains so the magnetization of each grain can be relatively independent of the magnetization of neighboring grains.[2] Decoupling the grains makes it possible for the dramatic magnetization transitions needed to distinguish between a "0" and a "1".

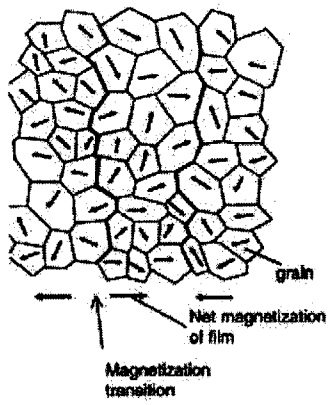

Figure 1[2]: Magnetized grains used as bits. No change in magnetization direction of grains corresponds to a "0". A dramatic change in magnetization direction corresponds to a "1".

Thus, it follows that in order to increase the storage efficiency of a device, more bits need to be packed into the same area. This requirement has two implications. Either a bit must have fewer grains or the sizes of the grains comprising a bit must shrink. Unfortunately, neither are viable options. Since the grains within a bit are only similarly magnetized – as opposed to being perfectly magnetized – a sizeable number of grains is needed to ensure a high signal-to-noise (SNR) ratio. At the same time, shrinking the grain size could leave the grains thermally unstable, i.e. their magnetizations could spontaneously change direction at room temperature. An unwanted change in magnetization effectively corrupts the data that is stored. Thermal instability occurs if

$$40k*T > K*V, \tag{1}$$

where k is the Boltzmann's constant, T is the temperature, K is the magnetic anisotropy and V is the volume of the grain. This equation suggests that one could just simply utilize a magnetic

material with a high K in order to prevent thermal instability. However, a write-head would struggle just to write the data since K is a measure of how easy it is to magnetize a material. As such, the three previously described interdependent scenarios present a quandary or more specifically, a "trilemma"[1].

One promising solution that has been proposed is the patterning of magnetic media, similar to how electronic circuit boards are patterned. With this method, a single bit of information is represented by a "grain island"[1] and opposing magnetizations would be recorded as a"1" or "0".Since grain islands are physically separated from one another, the transition noise is effectively minimized as there is a stark difference when bit magnetizations change. In addition, since the island bits would be composed of several grains that are exchanged coupled, the bits would enjoy a higher thermal stability.[1] Though the bits can be magnetized individually, the surface with all the bits behaves as if it were one unit. Consequently, the anisotropy constant and volume in equation 1 are now attributes of the bulk magnetic surface as opposed to just one bit.[3] Finally, a lower number of grains is needed to form one distinct bit than is needed in the conventional method. Thus, more bits can effectively be packed into storage devices than before. Figure 2 provides a visual representation of the differences between conventional media and patterned media.

This methodology could allow up to an areal density 4 Tbit/in^2, a whole order of magnitude over what previous technologies are able to accomplish.[1] In order to achieve this high density of data, the period of the island bits would have to be around 12 nm. (A period is defined as the diameter of one island plus the spacing between islands). Leading materials candidates for such an high areal density are Co systems such as Co/Pd or Co/Pt due to their "high perpendicular anisotropy and controllable magnetic properties." [4]

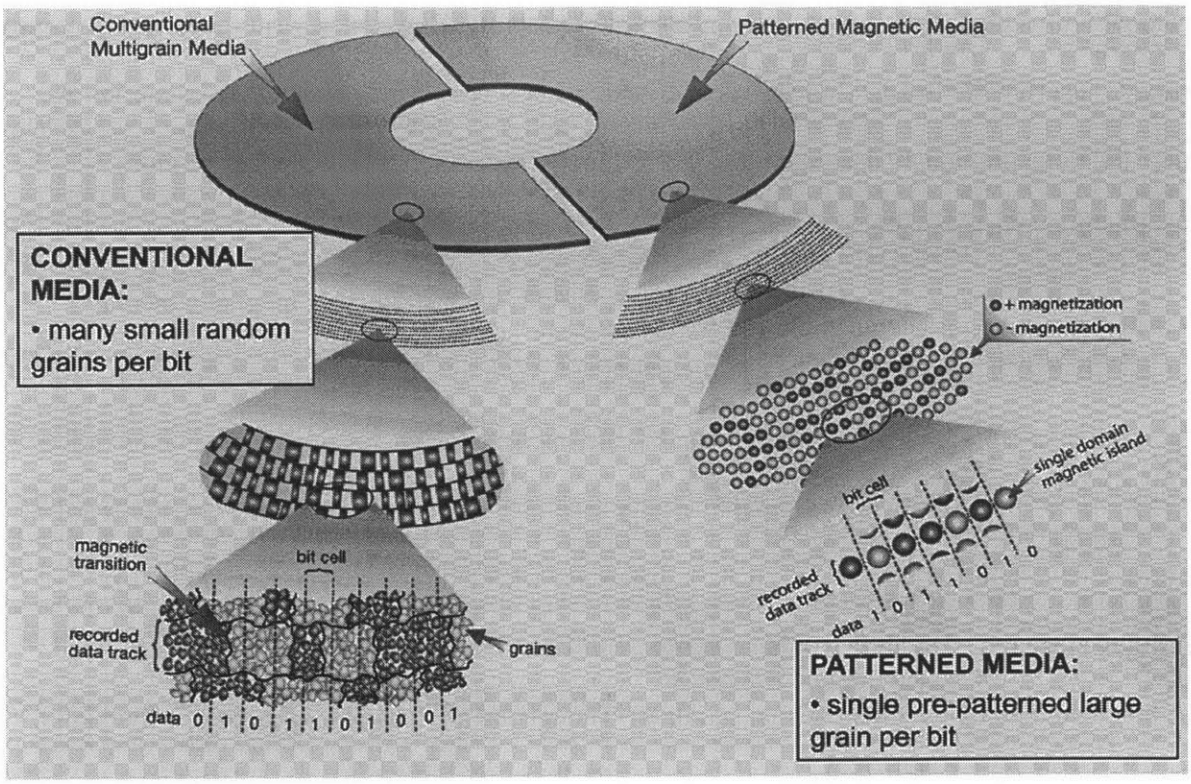

Figure 2[5]: Diagram comparing conventional media to patterned media.

1.2 Block- Copolymer Patterned Media

Various existing methods are available for patterning the surfaces of materials. One such method is photolithography. However, many of these fabrication methods are not suitable for the production components that are as small as the ones needed to store a high number of data bits on patterned media.

One promising method of forming these nanostructures involves the use of block copolymers(BCP).BCPs have a tendency to phase-separate into nano-sized structures and consequently, they are able to form interesting tunable morphologies over large areas.[6, 7] Once the desired pattern has been formed, the constituent polymers can then be etched away at varying

rates in order to inscribe and preserve the pattern on an underlying substrate. For patterned media, the underlying substrate would be the active magnetic layer.

BCPs are able to form these geometries because of their inherent incompatibility. From a thermodynamic standpoint, systems want to minimize their Gibbs free energy. The change in Gibbs free energy of mixing $\triangle G_{mix}$ for two homopolymers is governed by

$$\frac{\Delta G_{mix}}{k_b T} = \frac{f_a}{N_a}\ln(f_a) + \frac{f_b}{N_b}\ln(f_b) + f_a f_b \mathrm{X}_{ab}, \quad (2)$$

where k_b is the Boltzmann constant, T is the temperature, f and N are the respective volume fractions and degrees of polymerization of each constituent polymer and χ_{ab} is the Flory-Huggins parameter. A positive $\triangle G_{mix}$ ensures that the polymers will phase separate. To attain this positive $\triangle G_{mix,}$ high values of χ_{ab} and N are needed.

In response to a positive free energy of mixing, the segmented fragments of each polymer phase-separate and organize themselves at the nano-scale as a way to minimize "their free-energy cost of contact", described by χ_{ab}"[6] . In summary, this tendency to phase separate is dictated by the product $\chi_{ab}N$, known as the segregation strength.[8]

In addition to impacting the tendency for a BCP to phase separate, N also exerts a huge influence on the size of the nanostructures formed as a result of the separation. A smaller degree of polymerization corresponds to a smaller structure. In fact, the period D of the micro-domains formed is proportional to

$$\alpha N^{2/3} \chi^{1/6}, \quad (3)$$

where α is the characteristic length of a monomer unit.[6]

Thus, it follows that for the purposes of a patterning magnetic media, BCPs with high χ_{ab} and

low N is optimal. A high χ_{ab} ensures phase separation while a small N minimizes the period of micro-domains.

The exact morphology that results from the phase-separation is a function of the volume fraction of the two polymers that joined to form the BCP. For instance, in an A_nB_m copolymer, if n<<m, then spheres of A form in a matrix of B. However, if n~m, then a lamellar structure is formed.[2]. Even structures such as cylinders or more complex gyroids can be achieved by altering the volume ratio of the two polymers.[9]

However, there are alternative ways to control the pattern the BCP forms. For instance, the patterns are also tunable via processing conditions. Solvent annealing is one such condition. Jung and Ross showed that solvent annealing can be used to adjust component size, component spacing – two things that constitute the period – as well as the morphology the two polymers form when they phase-separate. As mentioned earlier, a high χN is needed to ensure that constituents polymers phase-separate on a substrate to begin with. This value can then be tempered accordingly to control how far apart the minority polymer domains are from one another. Solvent annealing is well suited for this purpose as it reduces the effectiveness of the Flory-Huggins parameter. In fact, the effective Flory-Huggins parameter χ_{ef} is given by

$$Xef=\chi(1-f_s). \quad (4)$$

χ is the interaction parameter if there were no solvent present, and f_s is the volume fraction of the solvent in the thin film.[10] The general idea is that the vapor from the solvent provides a screening effect between polymers and consequently lowers the equilibrium spacing between minority domains. Thus, the higher the vapor pressure from the solvent, the lower χ_{ef} and the lower the period length.

The individual domain sizes themselves can be tuned by the chemistry of the particular

solvent used to anneal the BCP. For example, Jung and Ross found that the width of the PDMS cylinders formed in a PS matrix decreased more quickly than the period length with increasing vapor pressure when toluene was the solvent. Since toluene is a partially selective solvent for PS, there is more swelling in PS than in PDMS. This problem can be remedied by using a mixture of two solvents to anneal the BCP. When they subjected the same co-polymer blocks to a mixture of toluene and heptane, the PDMS cylinder width increased. The increase can be attributed to the fact that heptane is a selective solvent for PDMS. Thus, it swells PDMS, causing an increase in its effective volume fraction. As the heptane volume fraction increases in the solvent, the resultant PDMS swelling can cause the cylindrical domains to give way to perforate lamellae and eventually to more disorganized morphology.[10]Evidently, vapor pressure is the main factor controlling period length while toluene/heptane ratio is the dominant factor controlling domain size.

However, it was found that vapor pressure also exerts a minor influence on morphology. Even with a high heptane fraction, cylindrical morphologies were observed as long as the net vapor pressure was low and a disorganized morphology was observed with low heptane fraction and high vapor pressure. The explanation provided by Jung and Ross holds that this behavior is due to the partial selectivity of toluene. "As the degree of PS swelling increases, an entropic effect resulting from the stretching may drive more toluene molecules into the PDMS block and therefore make toluene a less selective solvent."[10] Thus, toluene itself starts to swell its less preferred polymer PDMS. Similarly, cylindrical shapes are observed at low vapor pressures because there is just not enough solvent to cause swelling of the PDMS domains even with a relatively high concentration of PDMS-friendly heptane.

In addition, solvent-annealing serves another useful purpose. Not only are the right

morphology and appropriate domain size needed to make BCPs useful in patterning media, the formed pattern has to be sustained over a long range. Solvent annealing helps to promote the requisite long-range order.[9]

The final important part of the patterned media technique is the transferring of the patterns formed using BCPs onto a desired substrate. In order, to accomplish this goal, BCPs are gradually etched away. For this method to work, the two polymers comprising the BCP must have a sufficiently high etch-contrast. Thus, the polymer forming the matrix can be removed first so as to expose parts of an underlying magnetic layer. Through further etching, the lithographic "mask" formed by the remaining micro-domains can then be used to transfer the initial BCP pattern that was formed onto the magnetic layer.[7]

The sufficient etching contrast that is needed in order to make this technique viable is what makes PS-b-PDMS an ideal candidate for patterning magnetic media. When it's subjected to oxygen plasma during etching, a silicon-oxygen intermediate compound is formed. This resulting compound has a much higher etch resistance than PDMS alone, and consequently it is this intermediary compound that acts as a mask while the PS matrix is removed.[6]

1.3 Problem Statement

Thus far, one major challenge to patterning a magnetic substrate with BCP via using etching techniques has been intentionally negated. The desired pattern of PDMS spheres in a PS matrix is sandwiched between two thin PDMS layers, as shown in Figure 3. This formation is due to the varying surface tension between PS and PDMS. The surface tension of PDMS is 19.9 mN/m while that of PS is 40.7 mN/m [11]. Etching away the PDMS layer at the BCP/air interface as well as the PS matrix reveals the desired spherical morphology.[10]. In order to obtain distinct magnetic islands, the exposed Co that was previously underneath PS must be removed before the

intermediary silicon-oxygen compound is removed. However, the underlying PDMS layer could further impede the removal of the Co that is exposed once the PS matrix has been etched away.

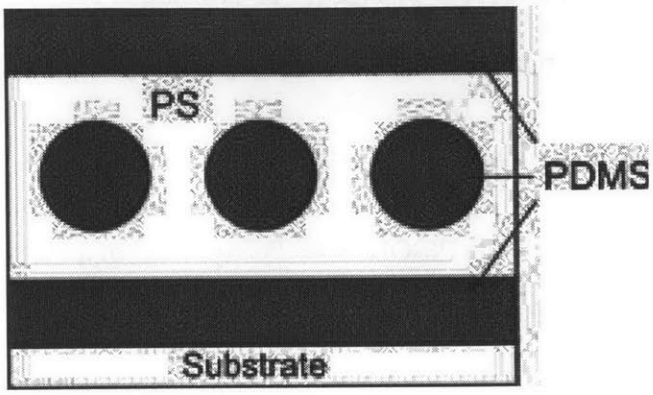

Figure 3[7]: Schematic of the layers formed after application of BCP with no PS brush.

O'Driscoll et.al demonstrated that brushing Si substrate with PS prevents formation of the PDMS wetting layer at the film/substrate interface. One of the primary aims of this study is to show that a good pattern can be obtained using a PS-OH brush on a Co substrate and to determine a range of optimal BCP thicknesses that can result in a well-defined pattern. A good pattern is characterized by uniform spherical shapes, long range order and lack of a PDMS wetting layer at the substrate/BCP interface. The second goal of the experiment is to investigate whether the removal of this PDMS layer results in a good pattern transfer onto the underlying Co substrate.

2. Materials & Methods

2.1 Sputter

Numerous rectangular Si wafers were cut from a thin wafer slice. The wafers measured approximately 1cm x 1cm and served as a substrate for the samples created for the purpose of the

experiment. The Si wafers were first cleaned with acetone to rid them of possible contaminants and subsequently air-dried. Then, a thin layer of Co was deposited on the substrates over a 30 s duration using a sputter gun in a vacuum chamber (~ air pressure of 10^{-7} atm). Co thickness is estimated to be approximately 6 nm based on the sputter gun's deposition rate.

2.2 Spin-Coating Block-Copolymer onto Substrate

All samples were brushed with PS-OH. Specifically, 50 μl of a 1% solution(by weight) of PS-OH(M_w=7000 kg) in PGMEA was spun-cast onto all samples at 3000 rpm and at an acceleration setting of 10,000 using a spin-coater manufactured by Headway Research Inc. Then, the brushed samples were thermally annealed at 170° C for 18 hours and then rinsed with toluene to rid them of excess PS-OH.

The BCP used was a 1% solution (by weight) of Poly(styrene-b-dimethylsilohexane) (M_n: PS(43000)-PDMS(8500); Mw/M_n=1.04) in cyclohexane. The PS-PDMS used to make the solution was supplied by Polymer Source Inc. It has a sample number of P3282-SDMS. 50 μl of this solution was spun-cast on each substrate for 30 seconds at varying rotational speeds and at accelerations chosen to achieve specific film thicknesses. Table 1 lists the spin-coating settings that correspond to varying film thicknesses. Care was taken to apply solution to substrates in a perpendicular fashion and to ensure that the solution was spun almost as soon as the entire sample was coated. Such practice enhanced the uniformity of the BCP coating. In order to determine the optimal settings that would yield the desired film thicknesses, plain Si wafers were coated with PS-PDMS and the thicknesses of coatings were measured using a Filmetrics F20 Thin-Film Analyzer. The polystyrene recipe was used to analyze the thickness of the BCP layer.

Table 1: Spin-Coating Settings for Samples

Thickness(nm)	Solution Concentration (Weight %)	Spin Speed(rpm)	Acceleration (unitless)
~27	0.66	4,000	10,000
~32	1	10,000	10,000
~35	1	7,000	10,000

2.3 Solvent Annealing

All samples were solvent-annealed in a sealed glass chamber using 3.25 ml of toluene and 0.65 ml of heptane in order to obtain a 5:1 ratio. This amount provides sufficient vapor pressure to selectively swell the PDMS domains and achieve the desired spherical shapes. Each sample rested on a beam connected to the side of the chamber. In addition, the chamber was connected to a gas flow system. Solvent vapor pressure within the chamber was indirectly controlled by introducing Nitrogen into the chamber as needed. Film swell thickness corresponds to increased vapor pressure since the film absorbs more solvent. Thus, the swell thickness serves as a quantitative gauge of solvent uptake. While the vapor pressure of the solvent was not measured, the Nitrogen flow rate corresponding to varying swell thicknesses was recorded and is shown in Table 2. The target solvent vapor pressure was gradually approached over the course of two minutes by varying the Nitrogen flow rate. Then, all samples were subjected to the target vapor pressure for thirteen minutes so as to allow for the polymers to equilibrate.

Table 2: Nitrogen Flow Rates Corresponding to Varying Thicknesses

Initial Thickness(nm)	Swell Thickness(nm)	N Flow Rate(Sccm)
32	80	3.00
35	50	10.00
35	65	7.00
35	80	3.25

2.4 Reactive Ion Etching (RIE) & Ion Milling

Samples were treated for 5s with a 15mTorr, 50W CF_4 plasma and for 22s with a 6mTorr, 90W O_2 plasma in order to remove the PDMS layer at the air/film interface and remove the PS matrix. Samples were sputter-etched using Ar and at 1.8×10^{-4} Torr.

2.5 Additional Information

In all, thirteen distinct samples were prepared. The first nine samples did not have a Co layer and were mainly prepared to test out which film thicknesses and swell thicknesses would result in a good pattern after RIE. Then, the parameters that produced the best results were used to prepare four more samples in order to verify that the same results would be observed once the Co layer was introduced. Table 3 lists all the samples with respective initial thicknesses and post-annealing thicknesses.

Table 3: Samples Prepared

Sample	Co Layer	Initial Thickness(nm)	Swell -Thickness(nm)
A	No	27	51
B	No	27	65
C	No	27	81
D	No	32	50
E	No	31	65
F	No	32	84
G	No	36	52
H	No	36	65
I	No	35	81
J	Yes	35	51
K	Yes	32	80
L	Yes	35	65
M	Yes	35	80

3. Results

Table 4: Period and Domain Size

Sample	Average Period Length(nm)	Average Domain Size(nm)
K	36.4(+/- 2.6)	20.8(+/- 5.2)
L	39.0(+/- 2.6)	20.8(+/- 2.6)
M	39.0(+/- 2.6)	18.2(+/- 2.6)

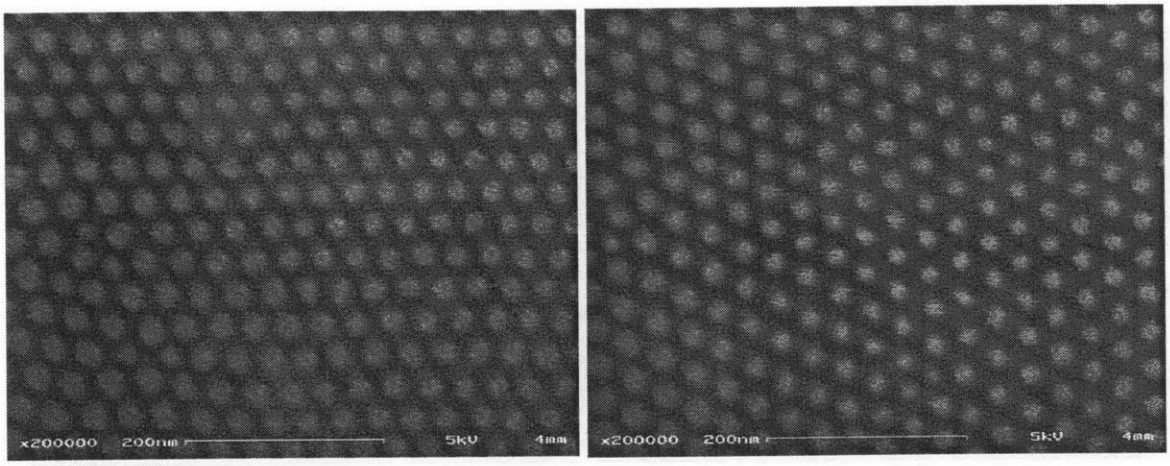

Figure 4: SEM Images of sample K after RIE.

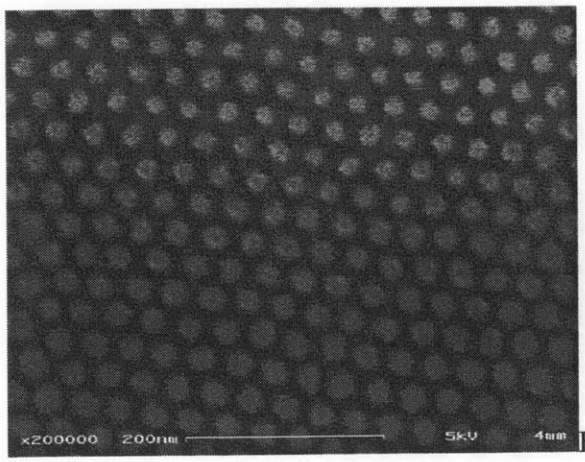

Figure 5: SEM Image of Sample L after RIE

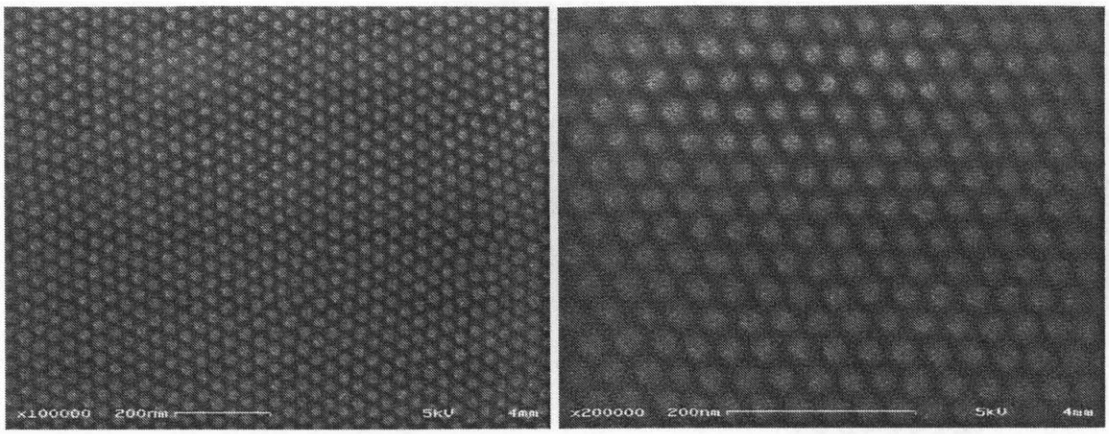

Figure 6: SEM Images of Sample M after RIE

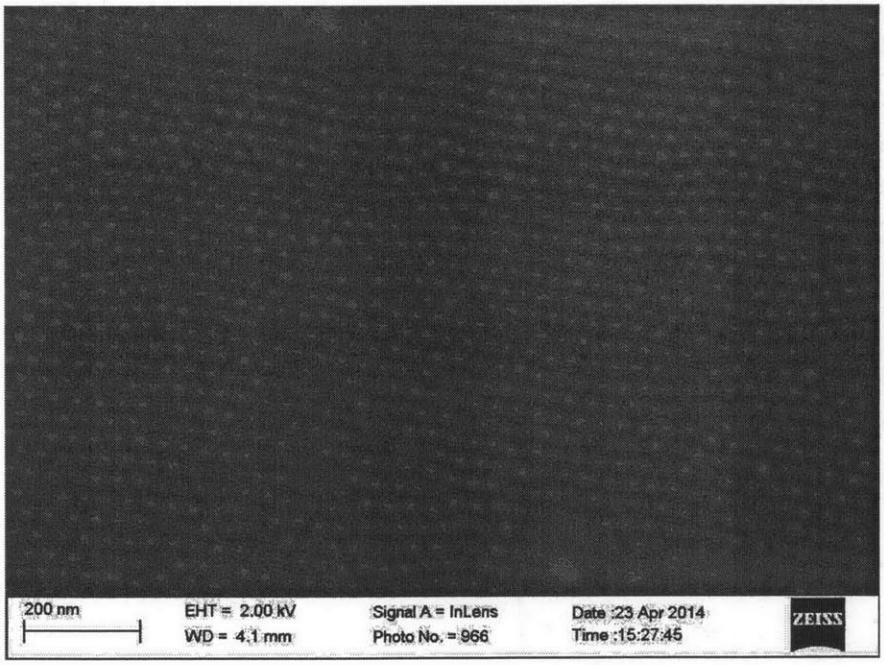

Figure 7: Sample M after Ion-Milling for 90s

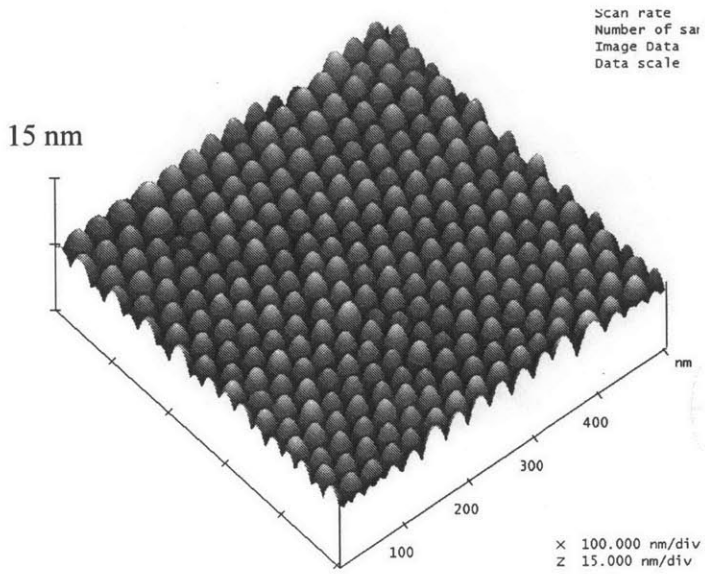

Figure 8: AFM Image of Sample M. Domain height ~ 4.4.5nm.

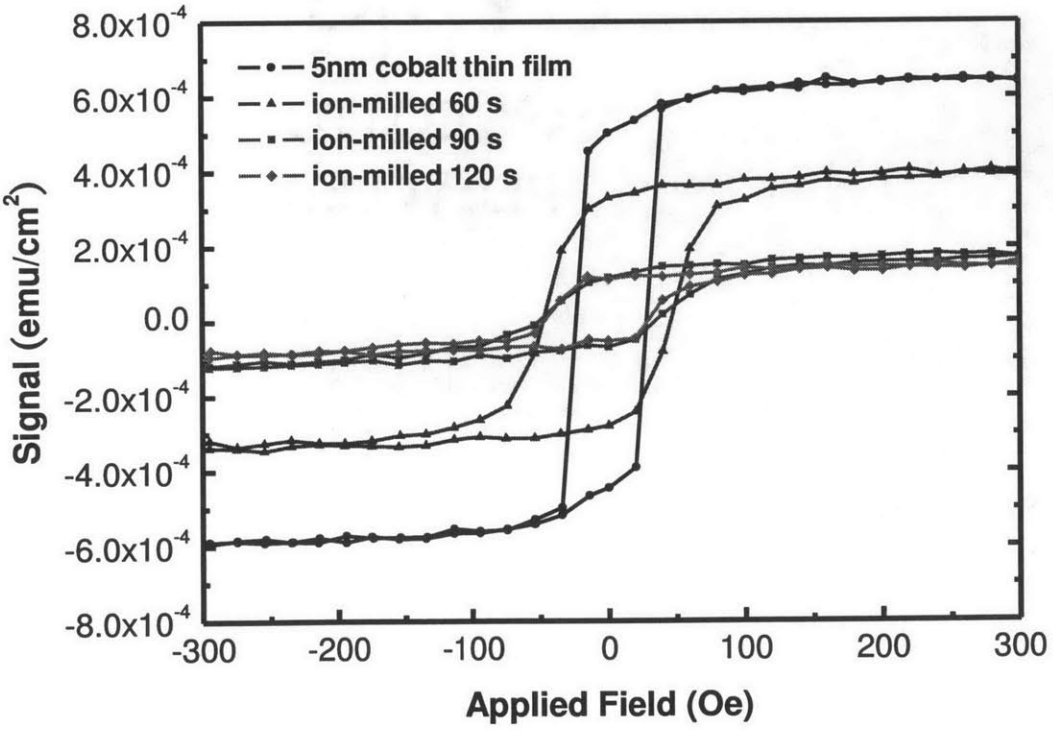

Figure 9: Hysteresis Loops for Sample M after Varying Ion-Milling durations

4. Discussion

As defined previously in the introduction, a good pattern must have good long-range order, i.e. domains of similar shapes must organize themselves in a very predictable pattern. Visual inspection shows that samples K, L and M all have very good long-range order. This long-range order is achieved due to the absorption of solvent during the annealing process. The annealing process ensures that the PDMS micro-domains are able to uniformly space themselves out. In addition, it ensures the robustness of the spherical morphology. Also, the significance of the duration of the solvent annealing cannot be understated. Giving samples enough time to equilibrate ensures the distinctiveness of the micro-domains that are formed.

Since samples with varying swell thicknesses yielded good patterns, it can be concluded that once a critical swell thickness is reached, additional solvent vapor pressure did not really help with the morphology. The smallest swell thickness of a sample shown in the results is 65 nm. While maintaining the initial BCP thickness, it is possible that smaller swell thicknesses, which correspond to less solvent vapor pressure and consequently less solvent uptake by the film, could still result in a good pattern. More experimentation is needed to ascertain the minimum swell thickness needed to achieve a good pattern for films that fall in the optimal BCP thickness range.

Based on the achieved results, it can be concluded that an optimal BCP thickness on a surface brushed with PS is in the range between 32 and 35 nm. This result was expected as it is consistent with an optimal BCP thickness reported by O'Driscoll et al. without the Co layer. It is worth noting that this optimal thickness is noticeably thinner than the thickness which O'Driscoll et al. recorded on a substrate not brushed with PS. This result was also expected and can be explained by the missing PDMS layer at the substrate/film interface. Since the substrate is

brushed with PS, the surface favors adherence by PS coming from the film as opposed to PDMS. RIE then etches all the PS in the substrate away to reveal some of the underlying Co and the end result is the desired mask without the PDMS wetting layer. The top PDMS layer is removed during RIE.

It is quite possible that the optimal thickness range for substrate brushed with PS and containing a Co underlayer could exceed 35 nm. The experiment only tested for initial film thicknesses up to and including 35 nm. However, based on the results, it can be reported that the film thickness needs to be at least 32 nm in order for a good pattern to be formed.

The periods of the patterns formed were between 36 and 39 nm with domain diameters between 18 and 21 nm. Similar results were observed by Jung and Ross in a study that used PS-b-PDMS(M_w=51.5 kg/mol) to pattern magnetic films. The authors were able to create patterns with an average period of 35.0 nm (+/- 1.5 nm) and average sphere diameter of17.9 nm (+/-1.1 nm).[12] Though the pattern dimensions observed in these two experiments are quite small, they are larger than the ideal period of 12nm that is needed to achieve an areal density of 4 Tbit/in^2, as discussed in the introduction. However, the observed periods are still on the same order of magnitude as the target period size. More experimentation is needed to figure out the best processing conditions that will yield component sizes as small as 12nm.

Figure 7 presents an image of sample M after it had been sputter-etched for 90s. This time duration was found to produce the best results but other images showing what the sample looks like after various ion-milling times can be found in the appendix. Qualitatively, the magnetic domains are boldly distinct from one another, which indicates a successful pattern transfer from the block-copolymer onto the Co substrate. The pattern formed on the thin Co film can be expected to have similar periodicity, long range order and morphology as sample M prior

to ion-milling. In addition, an AFM image of the sample – shown in Figure 8 – reveals that the domain height is 4-4.5nm, roughly half of the height reported by Jung and Ross in the aforementioned report.

Aside from the qualitative evidence of the pattern transfer, the hysteresis data (Figure 9) collected for the sample using a Vibrating Sample Magnetometer (VSM) confirms that the white domains shown in Figure 7 are indeed nano-sized Co domains. Two main pieces of information can be gathered from the hysteresis loops. First, the magnetic remanence (M_r) of the sample decreases with increasing ion-milling time. After RIE, PDMS domains as well as Co regions that were once underneath PS remain on the substrate. Ion-milling gradually etches away both these Co regions and the PDMS domains to expose the distinct Co islands beneath them. Since the process gradually rids the sample of some Co, the magnetic remanence decreases as more Co is removed from the sample. This trend is due to the fact that remanence is an extrinsic magnetic property, meaning its value is dependent on how much of a given material there is.

The second observation to be taken from the hysteresis plots is that the coercivity of the whole sample increases with increasing ion-milling time. Jung and Ross also observed the same changes in film coercivity when BCP patterns were transferred onto a thin Co film.[12] This behavior is also linked to the removal of large regions of Co and the simultaneous exposure of tinier Co domains. Large magnetic bodies tend to form several magnetic domains with varying magnetizations as a way of minimizing magnetostatic energy, which is a result of the stray magnetic field emanating from the material. However, the creation of domains and corresponding domain walls also has an energy penalty. While the magnetostatic energy increases in proportion with the volume (L^3) of a material, the domain wall energy increases with the area of the domain wall (L^2). [13]Thus, nucleation and growth of a domain wall is not worth the

associated energy for really small magnetic bodies. Such is the case for the Co domains shown in Figure 7.

Generally speaking, coercivities of single-domain particles tend to be higher since the entire particle has to be magnetized in one direction at once whereas for multi-domain particles, the domain wall gradually moves through the material and the material is gradually magnetized. Thus, the increased coercivity resulting from ion-milling further serves to confirm that small distinct Co islands were indeed created.

5.Conclusion

The goals of this experiment were to ascertain that good patterns suited for patterned media applications can be obtained on a Co substrate brushed with PS-OH and to transfer this pattern onto Co. The brush was instrumental in ridding the substrate of an undesired PDMS wetting layer that rested on top of the magnetic layer. A quality pattern, characterized by long-range order and domain uniformity, was achieved for BCP film thicknesses that were at least 32nm. In addition, this pattern was successfully transferred onto the Co layer, resulting in the fabrication of nano-sized magnetic domains. More research needs to be done on how to further reduce the domain size of the bits in order to maximize areal density. Additionally, it will be useful to investigate the magnetic behavior of individual "islands" as domain uniformity is critical to making bit-patterned media a truly viable technology. Of course, domain uniformity is a property that needs to be continuously improved.

6. Appendix

Sample M after being sputter-etched for 60s.

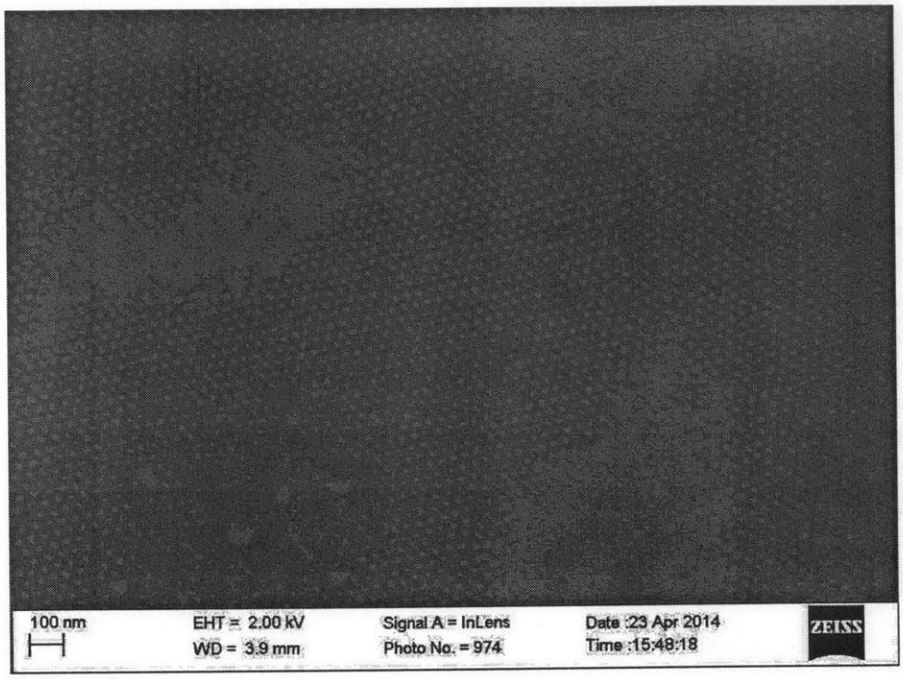

Sample M after being sputter-etched for 120s.

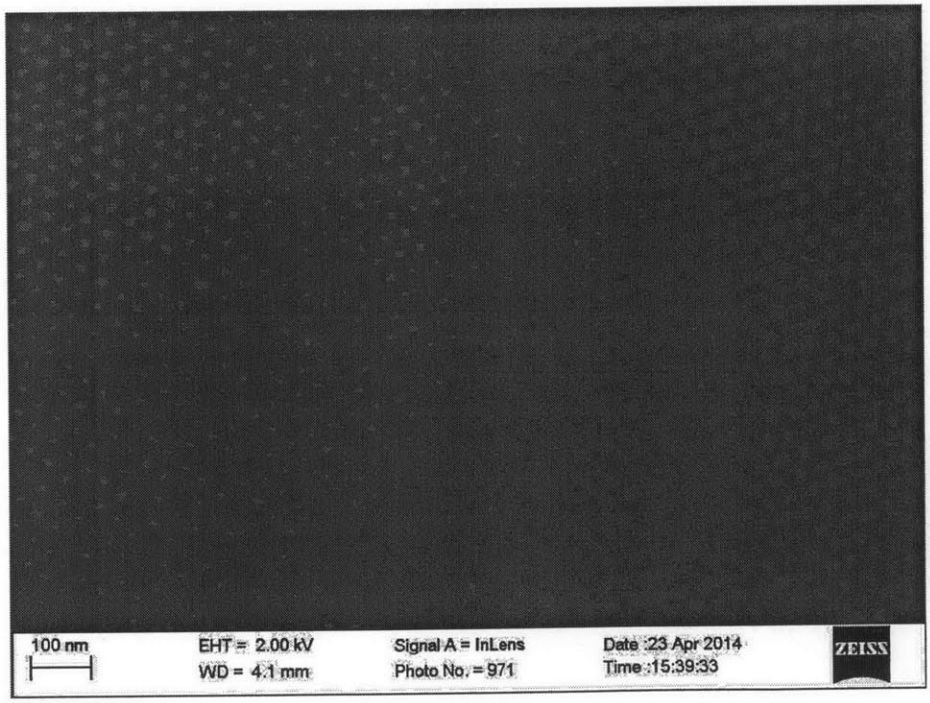

7. References

1. Ross, C. A. 3.15 Lecture 18: Data Storage. **2013**, *Online Lecture via MIT DMSE.*

2. Ross, C. A. PATTERNED MAGNETIC RECORDING MEDIA. *Annu. Rev. Mater. Res.* **2001**, *31*, 203-235.

3. Aravindakshan, V. Role of Bit Patterned Media in Future Hard Disk Drives, Massachusetts Institute of Technology, Cambridge, Ma, 2007.

4. Joel K W Yang and Yunjie Chen and Tianli Huang and Huigao Duan and Naganivetha Thiyagarajah and Hui Kim Hui and Siang Huei Leong and Vivian,Ng Fabrication and characterization of bit-patterned media beyond 1.5 Tbit/in 2. *Nanotechnology* **2011**, *22*, 385301.

5. Dobisz, E. A.; Bandic, Z. Z.; Tsai-Wei, W.; Albrecht, T. Patterned Media: Nanofabrication Challenges of Future Disk Drives <*br* />. *Proceedings of the IEEE* **2008**, *96*, 1836-1846.

6. Nunns, A.; Gwyther, J.; Manners, I. Inorganic block copolymer lithography. *Polymer* **2013**, *54*, 1269-1284.

7. O'Driscoll, B. M. D.; Kelly, R. A.; Shaw, M.; Mokarian-Tabari, P.; Liontos, G.; Ntetsikas, K.; Avgeropoulos, A.; Petkov, N.; Morris, M. A. Achieving structural control with thin polystyrene-b-polydimethylsiloxane block copolymer films: The complex relationship of interface chemistry, annealing methodology and process conditions. *European Polymer Journal* **2013**, *49*, 3445-3454.

8. Jung, Y. S. Templated Self-Assembly of Siloxane Block Copolymers for Nanofabrication, Massachusetts Institute of Technology, Cambridge, Ma, 2009.

9. Gu, W.; Xu, J.; Kim, J.; Hong, S. W.; Wei, X.; Yang, X.; Lee, K. Y.; Kuo, D. S.; Xiao, S.; Russell, T. P. Solvent-Assisted Directed Self-Assembly of Spherical Microdomain Block Copolymers to High Areal Density Arrays. *Adv Mater* **2013**, *25*, 3677-3682.

10. Jung, Y. S.; Ross, C. A. Solvent-Vapor-Induced Tunability of Self-Assembled Block Copolymer Patterns. *Advanced Materials* **2009**, *21*, 2540.

11. Jung, Y. S.; Ross, C. A. Orientation-Controlled Self-Assembled Nanolithography Using a Polystyrene−Polydimethylsiloxane Block Copolymer. *Nano Letters* **2007**, *7*, 2046.

12. Jung, Y. S.; Ross, C. A. Well-Ordered Thin-Film Nanopore Arrays Formed Using a Block-Copolymer Template. *Small* **2009**, *5*, 1654-1659.

13. Esterina, R. Commercialization of Bit-Patterned Media, Massachusetts Institute of Technology, Cambridge, Ma, 2009.